International Journal of Thermodynamics (IJoT)
ISSN 1301-9724 / e-ISSN 2146-1511
https://dergipark.org.tr/en/pub/ijot

Vol. 26 (No. 3), pp. 037-045, 2023
doi: 10.5541/ijot.1267822
Published online: September 1, 2023

Research Article

Calculation of the Phase Diagrams (T – X and T – P) and the Thermodynamic Quantities for the Solid – Liquid Equilibria in n-tridecane

[1]O. Tari, [2]*H. Yurtseven

[1] Department of Electrical and Electronics Engineering, Istanbul Arel University, 34537 Büyükçekmece, Istanbul - TURKEY
[2] Department of Computer Engineering, Baskent University, 06790 Ankara – TURKEY
E-mail: [2]*hamit@metu.edu.tr

Received 20 March 2023, Revised 26 May 2023, Accepted 28 July 2023

Abstract

The solid – liquid equilibria in n-tridecane is investigated by calculating phase diagrams and the thermodynamic quantities using the Landau phenomenological model. By expanding the free energy in terms of the order parameter of the solid phase, the phase line equations are fitted to the experimental data for the $T-X$ and $T-P$ phase diagrams from the literature. The temperature dependences of the thermodynamic quantities (order parameter ψ, susceptibility χ_ψ, free energy F, the heat capacity C, entropy S and the enthalpy H) are predicted for the n-tridecane from this model. Our results give that the slope $dT/dP \cong 2$ K/MPa for n-C_{13} to n-C_{17}. ψ varies with T as $\psi \sim (T-T_m)^{1/2}$ above T_m. It is linear for the ${\chi_\psi}^{-1}$, $S(T)$ and $C(T)$, and quadratic for the $F(T)$ and $H(T)$ in n-tridecane. This indicates that the Landau model, describes the observed behaviour of the phase diagrams satisfactorily for the solid – liquid equilibria in n-tridecane. Predictions of the thermodynamic quantities can also be compared with the measurements and predictions of some other theoretical models. The pressure effect, in particular, on the solid – liquid equilibria in n-tridecane can also be investigated under the model studied here.

Keywords: *Solid – liquid equilibria; $T-X$ and $T-P$ phase diagrams; thermodynamic quantities; n-tridecane.*

1. Introduction

The phase behavior of pure n-alkanes has been the subject of various experimental and theoretical studies. Experimental determination of thermodynamic and structural properties of pure long-chain n-alkanes, and phase diagrams of their molecular alloys have been reported in the literature as also indicated previously [1, 2]. Solid-liquid equilibria (SLE) of the n-alkanes [3] with the effect of pressure have been studied experimentally [4] and, the phase equilibria for the binary systems have been determined using a cryometric dynamic method at atmospheric pressure, additionally, the influence of pressure on liquidus curve up to 800 MPa was determined for systems [5]. A liquid to solid transition has been predicted by the high pressure molecular dynamics (MD) simulations [6], as also reported previously [7]. Various experimental studies [8-13] have been reported in the literature to explain the structure and the phase transitions of the rotator phases in n-alkanes. As stated some years ago, binary mixtures of normal alkanes exhibit a first order character of the liquid – solid transition [8 - 13], which has been studied by the Landau phenomenological theory [14]. It has also been indicated that binary normal alkane (n-alkane) shows the isotropic liquid state and the low temperature ordered crystal phase [15]. Experimentally, systematic hysteresis has been observed by photopyroelectric calorimetry confirming the first order behavior of n-alkanes [16]. The crystallization and phase transition behaviours of normal alkane (n-docosane) were studied by the DSC, XRD and variable – temperature solid state NMR [17]. Also, pressure – induced phase changes of n-heptane have been studied experimentally [7]. Recently, theoretically by means of the molecular dynamic simulations, thermodynamic properties of small linear alkanes have been studied [18]. Experimentally, for the tetradecane + hexadecane system the $T-X$ phase diagram was obtained at various pressures [1, 19]. Also, the experimental measurements were conducted for the phase diagrams of the n-tridecane + n-hexane (n-cyclohexane) systems [20]. The equilibrium phase diagram of n-octadecane + n-nonadecane has been studied [21].

Regarding the phase diagrams for the binary systems, the alkane system of dodecane-tridecane has been obtained to find phase change materials (PCMs) for freezing applications [22]. Also, the phase diagram for the binary systems of $n-C_{11}\cdots\cdots$ was experimentally investigated to employ potential PCMs for cryogenic materials [23]. The equilibrium phase behaviours and thermal characteristics (phase diagrams, enthalpies, melting / freezing temperatures) of the binary systems were experimentally investigated [24].Very recently, we have also studied the liquid – solid phase diagram of n-alkanes (C_nH_{2n+2}) [25] and the thermodynamic properties of the binary system of tetradecane and hexadecane [26, 27] by using Landau mean field theory which has also been used to describe the liquid – solid transitions in n-alkanes in some previous studies [14, 28]. Since adequate thermodynamic models can describe the

*Corresponding Author

phase behavior of the very complex systems such as pure n-alkanes and synthetic mixtures by knowing their structural properties [1], the Landau model can be an appropriate one to describe the observed behavior of those mixtures. As indicated previously, the main aim is to further understand the complexity of the phase stability and the phase transition of n-alkanes [17]. In order to describe the thermal characteristics of the solid-liquid transition in n-alkanes generally their common physical properties can be investigated by modelling them theoretically. This can provide an universal curve for their phase diagrams ($T - T_m$ vs. $x_m - x$ or $T - T_m$ vs. $P - P_m$) and also for their thermodynamic quantities close to the liquid-solid transitions in n-alkanes. This has motivated us to investigate the liquid – solid transition on the phase boundary between the liquid phase and the two-phase liquid – solid phase domain, particularly, in n-tridecane within the Landau phenomenological model. $T - X$ and $T - P$ phase diagrams of n-tridecane are calculated by means of the phase line equation which is fitted to the experimental data [4]. Based on the phase diagrams calculated, the temperature dependences of the thermodynamic quantities such as the order parameter, susceptibility, free energy, entropy, heat capacity and enthalpy are predicted for n-tridecane.

2. Theory

The solid – liquid phase equilibria in synthetic waxes can be studied by the Landau mean field theory. By expanding the free energy of the solid phase in terms of the order parameter, the phase line equation and the order parameter can be obtained by means of the coefficients in the expansion. From the free energy expansion, thermodynamic functions of interest can be obtained for the solid – liquid equilibria in those mixtures.

2.1 Phase Line Equation and the Order Parameter

We can express the free energy of the solid – liquid phase equilibria in synthetic waxes which exhibit first order transition, in terms of the order parameter on the basis of the Landau phenomenological model as

$$F = a_2\psi^2 + a_3\psi^3 + a_4\psi^4 \tag{1}$$

where the coefficients a_2, a_3 and a_4 can depend on the temperature, concentration (mole fraction) and pressure in general. Note that there is no ordering in the liquid phase so that the free energy of this phase is zero ($F_L = 0$). Various forms of the free energy expanded in terms of the order parameters including the coupled terms for the rotator phases in n-alkanes, have been given in some previous studies [14, 28]. We have also given the functional form of the free energy in terms of the order parameters for n-alkanes in our recent studies [25-27].

The free energy can be minimized with respect to the order parameter ψ of the solid phase ($\partial F/\partial\psi = 0$), which gives

$$4a_2\psi^2 + 3a_3\psi + 2a_2 = 0 \tag{2}$$

By solving Eq. (2.2) for ψ, we get

$$\psi = \left(-3a_3 \pm \sqrt{9{a_3}^2 - 32a_2a_4}\right)/8a_4 \tag{3}$$

In the root square, by assuming that

$$(32a_2a_4/9{a_3}^2) \ll 1 \tag{4}$$

using the Taylor's expansion

$$(1-x)^n = 1 - nx + \frac{n\,(n-1)}{2!}x^2 + \cdots \tag{5}$$

the order parameter ψ becomes

$$\psi = -\frac{3a_3}{8a_4} \pm \frac{3a_3}{8a_4}\left(1 - \frac{16}{9}\frac{a_2a_4}{{a_3}^2}\right) \tag{6}$$

where only the first two terms in Eq. (5) are taken into account (higher order terms are ignored). By also taking the positive root solution (Eq. (6)), the order parameter can be written simply as

$$\psi = -\frac{2a_2}{3a_3} \tag{7}$$

This can express the temperature and pressure dependence of the order parameter in the solid phase for the solid – liquid equilibria in synthetic waxes. In order to get the phase line equation for the solid – liquid transition, the order parameter ψ (Eq. (7)) can be substituted into the free energy (Eq. (1)) which gives

$$a_2a_4 = -3{a_3}^2/4 \tag{8}$$

This is the phase line equation for the solid – liquid equilibria in synthetic waxes. By considering temperature, concentration or pressure dependence of the coefficients a_2, a_3 and a_4, $T - X$, $T - P$ or $P - X$ phase diagrams of those compounds can be predicted by the Landau mean field theory using the experimental data. In this study, we calculated $T - T_m$ versus $x_m - x$ (T_m and x_m are the melting temperature and composition, respectively) and $T - T_m$ versus $P - P_m$ (P_m denotes the melting pressure) for the liquid-solid transition in n-tridecane by using the experimental data [4].

2.2 Thermodynamic Quantities

For the solid – liquid equilibrium in synthetic waxes, the temperature dependence of the thermodynamic quantities such as the order parameter susceptibility, entropy, enthalpy, heat capacity and the free energy can be predicted from the Landau phenomenological model.

The order parameter susceptibility (χ_ψ) can be obtained from the free energy (Eq. (1)) in terms of the order parameter ψ for the solid – liquid equilibria in synthetic waxes. By using the definition of the susceptibility, ${\chi_\psi}^{-1} = \partial^2F/\partial\psi^2$, we find that

$${\chi_\psi}^{-1} = 2(a_2 + 3a_3\psi + 6a_4\psi^2) \tag{9}$$

or by using ψ (Eq. (7)) in this equation, the inverse susceptibility becomes

$${\chi_\psi}^{-1} = -2a_2 + \frac{16}{3}\frac{{a_2}^2a_4}{{a_3}^2} \tag{10}$$

As in the order parameter ψ, by means of the dependences of the coefficients a_2, a_3 and a_4, the order parameter susceptibility χ_ψ can be obtained as functions of temperature, pressure and concentration for the solid – liquid

Table 1. Values of the coefficients (Eq. (15)) at the melting pressure ($P = P_m = 0.1\ MPa$) with the melting temperatures (T_m) and composition (x_m) of M_1 to M_9 [4] of the various mixtures (n-C_{13} to n-C_{17}) for the liquid – solid transition in n-tridecane. Uncertainties of the coefficients and the R^2 values are also given.

Mixtures	Melting Temperature T_m (K)	Melting composition x_m (mass %)	$-a_o'$ (K)	$-a_1'$ K/(mass %)	$-a_2' \times 10^{-1}$ K/(mass %)^2	$-a_3' \times 10^{-3}$ K/(mass %)^3	R^2
n-C_{13}	270.6	50.02	41.3±8.4	5.43±0.94	2.18±0.33	3.10±0.38	0.9991
n-C_{14}	270.6	49.98	39.1±7.9	5.21±0.90	2.11±0.32	3.02±0.36	0.9991
n-C_{15}	273.7	33.33	7.5±3.3	2.24±0.69	-1.55±0.43	4.88±0.86	0.9996
n-C_{16}	277.0	25.4	10.4±3.3	4.17±1.07	4.03±1.05	16.83±3.19	0.9996
n-C_{17}	279.9	20.13	-3.5+0.5	-0.75±0.22	-2.21±0.30	2.22±1.32	1

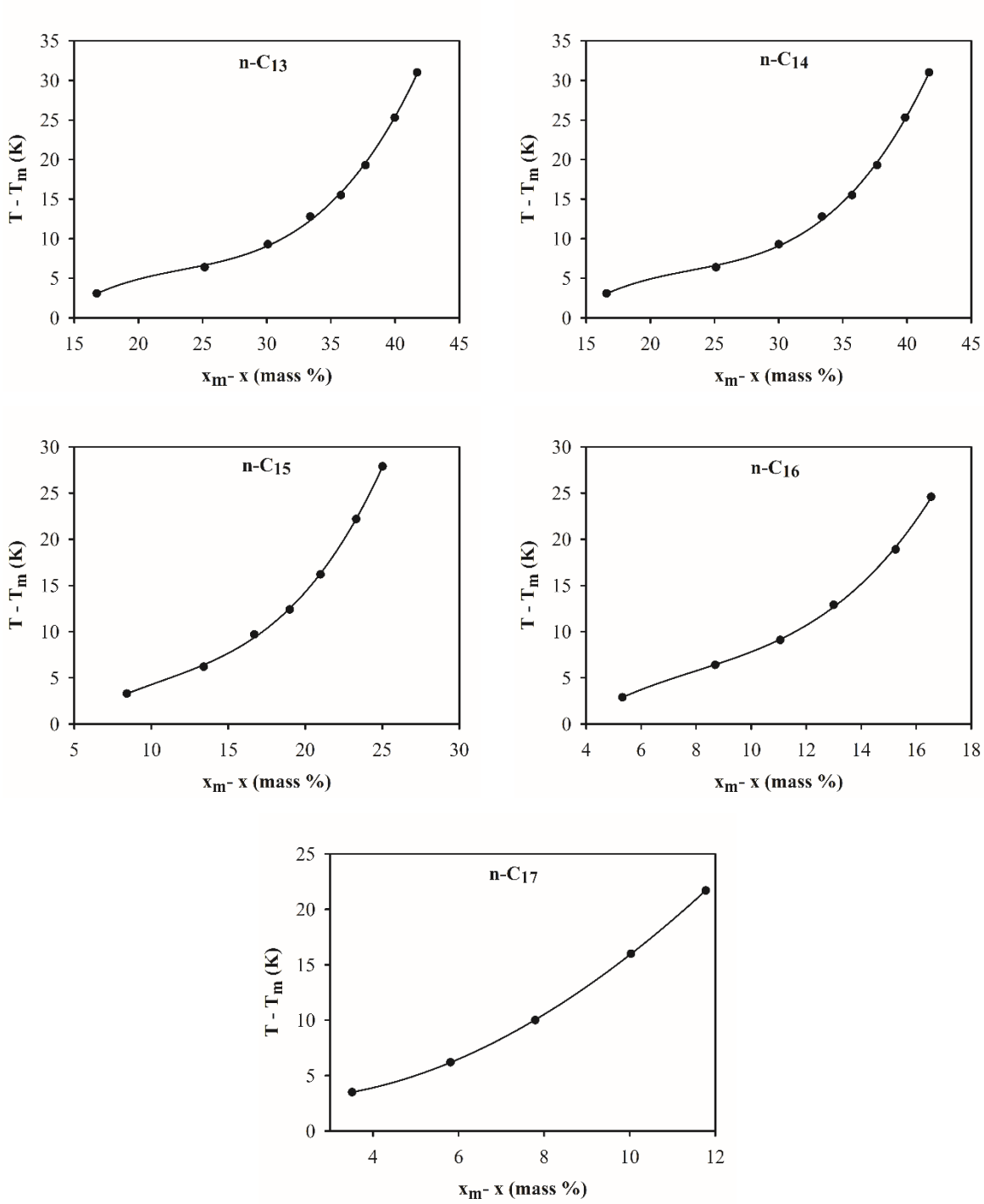

Figure 1. $T - X$ phase diagram of liquid – solid phase transition in n-tridecane of various mixtures according to Eq. (15). T_m and x_m indicate the melting temperature and composition (mass %), respectively, ($P = P_m$) with the experimental data [4] as shown.

equilibria in synthetic waxes. The temperature dependence of the other thermodynamic quantities can also be predicted which is given below. As we have calculated the thermodynamic quantities of the binary system of tetradecane and hexadecane for its liquid-solid phase transition previously [26], we also calculated in this study the order parameter, inverse susceptibility, free energy, entropy, heat capacity and the enthalpy as a function of $T - T_m$ for n-tridecane.

Table2. Values of the coefficients (Eq. (15)) at the melting composition ($x = x_m$) with the melting temperatures (T_m at $P = 0.1\ MPa$) of various components M_1 to M_9 [4] for the liquid – solid transition in n-tridecane. Uncertainties of the coefficients and the R^2 values are also given.

Mixtures	T_m (K)	$a_o' \times 10^{-1}$ (K)	$a_4' \times 10^{-1}$ (K/MPa)	R^2
M_1	270.6	3.21 ± 2.12	1.99 ± 0.03	0.9987
M_2	273.7	3.67 ± 2.22	1.95 ± 0.04	0.9986
M_3	277.0	4.13 ± 2.90	1.91 ± 0.05	0.9975
M_4	279.9	3.51 ± 2.75	1.90 ± 0.05	0.9977
M_5	283.4	2.96 ± 1.85	1.88 ± 0.03	0.9989
M_6	286.1	3.41 ± 2.31	1.94 ± 0.04	0.9984
M_7	289.9	3.45 ± 2.68	1.92 ± 0.04	0.9979
M_8	295.9	2.48 ± 1.84	1.95 ± 0.03	0.9990
M_9	301.6	1.21 ± 1.14	1.97 ± 0.02	0.9996

3. Calculations and Results

3.1 Calculation of Phase Diagram

In this study, we first obtained the phase diagrams ($T - P$ or $T - X$) for the solid – liquid equilibria in synthetic waxes. This was done by assuming the temperature, pressure and concentration (mole fraction) of the coefficients a_2, a_3 and a_4 as Eqs. (1) - (4).

$$a_2 = a_{20} + a_{21}(T - T_m) + a_{22}(P - P_m) \tag{11}$$

$$a_3 = a_{30}(T - T_m)^{1/2} \tag{12}$$

$$a_4 = a_{40} + a_{41}(x - x_m) + a_{42}(x - x_m)^2 + a_{43}(x - x_m)^3 \tag{13}$$

where T_m, P_m and x_m represent the melting (freezing) temperature, pressure and concentration, respectively. By substituting those dependences (Eqs. (11) - (13)) into the phase line equation (Eq. (8)), one gets

$$[a_{20} + a_{21}(T - T_m) + a_{22}(P - P_m)][a_{40} + a_{41}(x - x_m) + a_{42}(x - x_m)^2 + a_{43}(x - x_m)^3] = -\frac{3}{4}a_{30}{}^2(T - T_m) \tag{14}$$

By expanding the parenthesis and ignoring the cross terms such as $(T - T_m)(x - x_m)$ and $(P - P_m)(x - x_m)$ with the higher order terms in the expansion, we find that

$$T - T_m = a_0' + a_1'(x - x_m) + a_2'(x - x_m)^2 + a_3'(x - x_m)^3 + a_4'(P - P_m) \tag{15}$$

where

$$a_0' = a_{20}a_{40}/a_0$$
$$a_1' = a_{20}a_{41}/a_0$$
$$a_2' = a_{20}a_{42}/a_0$$
$$a_3' = a_{20}a_{43}/a_0$$
$$a_4' = a_{22}a_{40}/a_0 \tag{16}$$

with the definition of a_0 as

$$a_0 = -1/(a_{21}a_{40} + 3\,a_{30}{}^2/4) \tag{17}$$

We plot in Fig. 1 the $T - T_m$ versus $x_m - x$ (mass %) phase diagrams of n-paraffins ranging from n-C_{13} to n-C_{17} with various number of compounds at $P = P_m = 0.1$ MPa (atmospheric pressure) by using the experimental data [4] according to Eq. (15). From this fit, we obtained values of the coefficients a_0', a_1', a_2' and a_3', which are given in Table 1. For the determination of the coefficients a_0', a_1', a_2', a_3' and a_4', our fitting procedure is the following: according to Eq. (15), by taking $P = P_m = 0.1$ MPa we obtained $T - T_m$ as a function of $x - x_m$ in the polynomial form, which was fitted to the experimental data [4] to determine the coefficients a_0', a_1', a_2' and a_3'. Similarly, by taking $x = x_m$ in Eq. (15) which was fitted to the experimental data [4] and the coefficients a_0' and a_4' were determined, as given in Table 1. Values of the uncertainties with the R^2 values are also indicated at Table 1. Melting temperatures were taken at $P = 0.1$ MPa by using the observed $P - T$ data [4]. The melting temperatures and compositions at $P = 0.1$ MPa are given at Table 1 for the mixtures (n-C_{13} to n-C_{17}) from the observed data [4]. At the melting composition ($x = x_m$) from Eq. (15), variation of $T - T_m$ with the $P - P_m$ was obtained by using the observed data [4] for various mixtures (M_1 to M_9) for the liquid-solid phase transition in n-tridecane, as plotted in Fig. 2. Coefficients of a_0' and a_4' with the uncertainties and the R^2 values are given at Table 2.

3.2 Calculation of the Order Parameter and Susceptibility

Temperature dependence of the order parameter ψ for the solid – liquid equilibria in synthetic waxes can be obtained using Eq. (7) by means of Eqs. (11) and (12), as stated above. By substituting Eqs. (11) and (12) into Eq. (7) at the melting pressure ($P = P_m$), we get simply

$$\psi = \psi_0(T - T_m)^{1/2} \tag{18}$$

In our treatment, we ignored the $(T - T_m)^{-1/2}$ term in the expansion since the order parameter of the solid phase decreases and goes to zero as the melting temperature T_m is approached from the solid phase (ψ is zero in the liquid phase). We used the experimental data from the $P - T$ measurements of the mixtures M_1 to M_9 in n-tridecane at $P = 0.1$ MPa to calculate the order parameter ψ according to Eq. (18). We plot in Fig. 3 the order parameter ψ (normalized) as a function of the $T_m - T$ for the mixtures M_1 to M_9 in n-tridecane ($P = 0.1$ MPa).

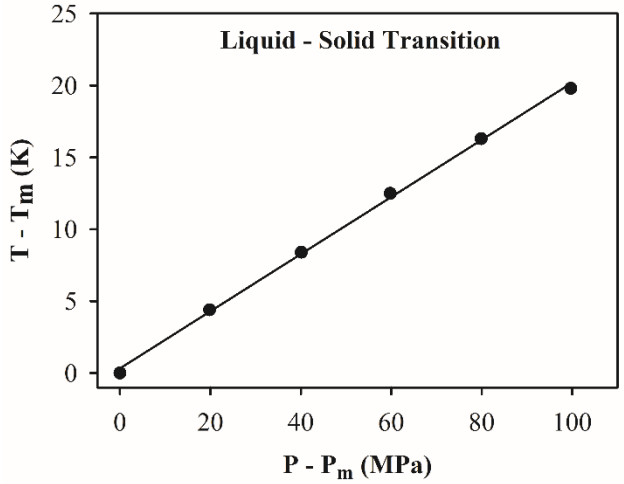

Figure 2. Liquid – solid phase transition temperatures of components (M_1 to M_9) in n-tridecane as a function of pressure according to Eq. (15) at $x = x_m$. T_m and P_m represent the melting temperature and pressure, respectively, with the experimental data [4] shown.

Similarly, temperature dependence of the order parameter susceptibility (χ_ψ) can be obtained as we obtained for ψ (Eq. (18)). By substituting Eqs. (11) – (13) into Eq. (10), we get the temperature and pressure dependence of ${\chi_\psi}^{-1}$ at $x = x_m$ as

$${\chi_\psi}^{-1} = A + B(T - T_m) + C(P - P_m) + D(T - T_m)^{-1} \quad (19)$$

where

$$A = \frac{2a_{20}}{{a_{30}}^2}(2a_{21}a_{40} - {a_{30}}^2)$$
$$B = -\frac{2a_{21}}{{a_{30}}^2}({a_{30}}^2 - a_{21}a_{40})$$
$$C = \frac{a_{22}}{{a_{30}}^2}({a_{30}}^2 - a_{21}a_{40})$$
$$D = \frac{2a_{20}a_{40}}{{a_{30}}^2}[a_{20} + a_{22}(P - P_m)] \quad (20)$$

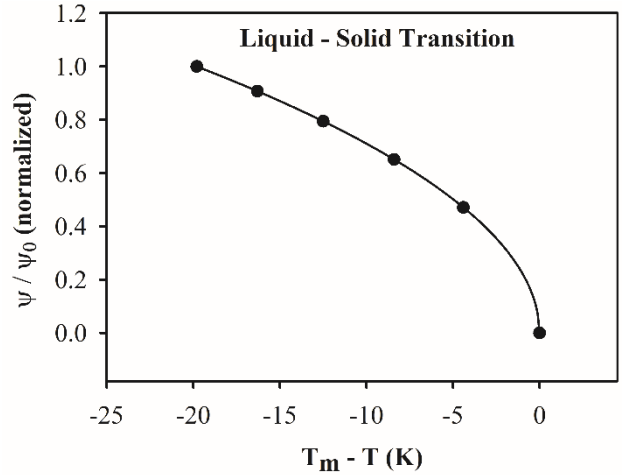

Figure 3. Temperature dependence of the order parameter ψ (normalized) for the solid phase, which was calculated according to Eq. (18) at the melting composition ($x = x_m$) using the temperatures, T_m, melting temperatures [4] for liquid – solid transition of various components (M_1 to M_9) of n-tridecane.

Note that the order parameter susceptibility (χ_ψ) can also be calculated directly from the temperature dependence of the order parameter ψ (Eq. (18)) according to Eq. (9) using Eqs. (11) – (13). By means of Eqs. (11) – (13) at $x - x_m$ ($P = P_m = 0.1$ MPa) we simply obtain

$${\chi_\psi}^{-1} = {\chi_0}^{-1}(T - T_m) \quad (21)$$

when we take $a_{20} = 0$, where

$${\chi_0}^{-1} = (16{a_{21}}^2 a_{40}/3\,{a_{30}}^2) - 2a_{21} \quad (22)$$

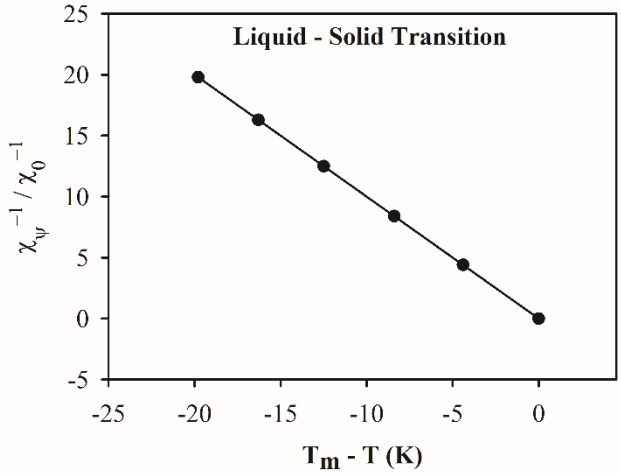

Figure 4. Temperature dependence of the inverse susceptibility ${\chi_\psi}^{-1}$ (normalized) for the order parameter ψ, which was calculated according to Eq. (21) at the melting composition ($x = x_m$) using the temperatures, T_m, melting temperatures [4] for liquid – solid transition of various components (M_1 to M_9) of n-tridecane.

In this study, the temperature dependence of ${\chi_\psi}^{-1}$ was calculated at $P = P_m = 0.1$ MPa according to Eq. (19) by ignoring the $(T - T_m)^{-1}$term since the inverse susceptibility decreases as the melting temperature T_m is approached from the solid phase for the liquid – solid transitions, in particular, n-tridecane studied here. We plot in Fig. 4 the inverse susceptibility (${\chi_\psi}^{-1}$) normalized as a function of the $T_m - T$ for the mixtures M_1 to M_9 in n-tridecane ($P = 0.1$ MPa). As seen from Fig. 4 it is a single curve at various $T_m - T$ for those mixtures (M_1 to M_9) in n-tridecane.

3.3 Calculation of the Free Energy, Entropy, Enthalpy and Heat Capacity

We assumed the temperature dependence of the free energy in the functional form.

$$F = F_0(T - T_m)^2 \quad (23)$$

for the solid – liquid transition for the mixtures M_1 to M_9 in the n-tridecane ($P = 0.1$ MPa). Fig. 5 gives F (normalized) at various $T - T_m$ as a single curve. This results in the entropy $S = (\partial F/\partial T)_V$, which varies linearly variation with the temperature as

$$S = S_0(T - T_m) \quad (24)$$

We plot the entropy (normalized) as a function of $T - T_m$ in Fig. 6.

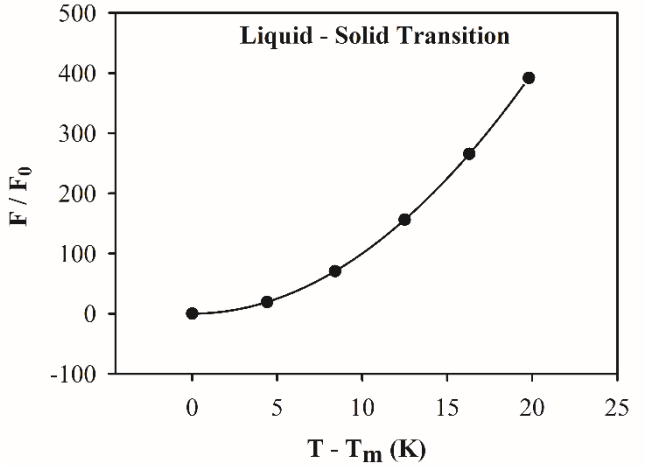

Figure 5. Temperature dependence of the free energy F (normalized) for the solid phase, which was calculated according to Eq. (23) at the melting composition ($x = x_m$) using the temperatures, T_m, melting temperatures [4] for liquid – solid transition of various components (M_1 to M_9) of n-tridecane.

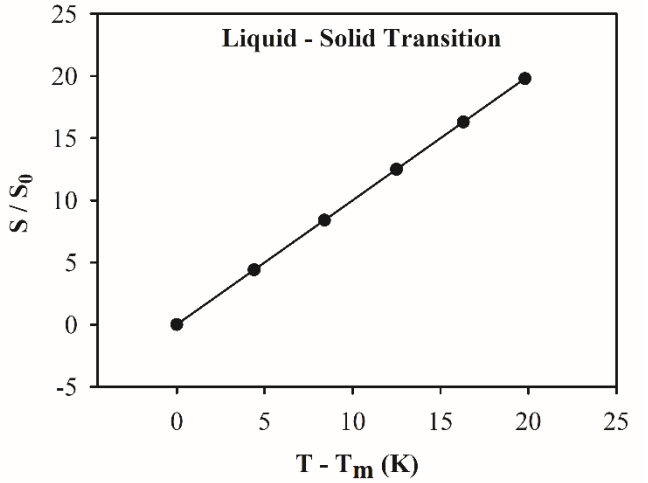

Figure 6. Temperature dependence of the entropy S (normalized) for the solid phase, which was calculated according to Eq. (24) at the melting composition ($x = x_m$) using the temperatures, T_m, melting temperatures [4] for liquid – solid transition of various components (M_1 to M_9) of n-tridecane.

Using the definition of the heat capacity $C_V = T(\partial S/\partial T)_V$, we obtain from Eq. (23),

$$C = C_0 T \tag{25}$$

where $C_0 = S_0$, as the linear variation of C with the temperature similar to the entropy S. We plot in Fig. 7 the heat capacity C (normalized) as a function of $T - T_m$ (above the melting temperature) for the various mixtures (M_1 to M_9) in the synthetic waxes. Finally, from the definition of $C_V = \partial H/\partial T$, we obtained the enthalpy function as

$$H(T) - H(T_m) = H_0\left(T^2 - {T_m}^2\right) \tag{26}$$

where $H_0 = S_0/2$. This is plotted in Fig. 8 for the solid – liquid transition in the mixtures studied.

4. Discussion

In this study, the $T - X$ and $T - P$ phase diagrams were calculated by means of the Landau phenomenological model using the experimental data [4] for composition (mass %) of the various mixtures (M_1 to M_9) for the solid – liquid equilibria of n-tridecane (n-C_{13} to n-C_{17}). As given in the $T - T_m$ versus $x_m - x$ plots (Fig. 1), the composition (mass %) increases below the melting composition (x_m) for all the components of n-tridecane as we fitted Eq. (15) to the experimental data at $P = P_m$. The cubic polynomial fit (Eq. (15)) is reasonable to describe the experimental data for the variation of the liquid – solid transition temperatures with the composition below the melting point in various mixtures (M_1 to M_9) for n-tridecanes (n-C_{13} to n-C_{17}) on the basis of the Landau mean field model. Since the experimental data were insufficient for the mixtures n-C_{18} to n-C_{24} [4], we were not able to perform the fitting procedure for the three mixtures. We also fitted Eq. (15) to the experimental $P - T$ data [4] at the melting composition ($x = x_m$) for mixtures (M_1 to M_9) to describe the liquid – solid phase transitions in complex waxy systems, as plotted in Fig. 2. As a single curve, variation of $T - T_m$ with the $P - P_m$ is linear (Eq. (15)) at $x = x_m$ for the pressure range (0.1 to 100 MPa) of those mixtures, which was also obtained experimentally [4] for the $T - P$ phase diagram.

Regarding the change in the temperature $(T - T_m)$ per unit change in the composition $(x_m - x)$, which gives rise to the slope, $d(T - T_m)/d(x_m - x)$ in the $T - T_m$ versus $x_m - x$ plot above the melting point, we find an almost linearity in the temperature range of ~15 - 20 K which corresponds to the composition range of 35 - 40 (mass %) for the mixtures of n-C_{13}, n-C_{14} and n-C_{15} (Fig. 1). This gives the slope value of ~2 K/mass (%) with the components of M_6 to M_9 (n-C_{13} and n-C_{14}), M_7 to M_9 (n-C_{15}). For the components of M_8 and M_9 (n-C_{16}), and M_7 to M_9 (n-C_{17}), within the range of 15 – 25 K (13 – 16 mass %) and 10 – 22 K (8 – 12 mass %), respectively, the slope value is about 3 K/mass (%). Outside this range of the temperature and the composition (mass %) above the melting point, changes in the temperature $(T - T_m)$ and in the composition $(x_m - x)$ are nonlinear so that the slope change corresponds to the heavier components in the composition (mass %) of M_1 to M_5 in n-tridecane (n-C_{13} to n-C_{17}), as shown in Fig. 1. We expect the same kind of behavior for the mixtures of n-C_{18} and n-C_{19} whose slope changes nonlinearly in the $T - T_m$ versus $x_m - x$ plot. For those two mixtures, we were not able to predict the variation of $T - T_m$ with the $x_m - x$ because of the lack of the experimental data [4], as stated previously.

Variation of the temperature change $(T - T_m)$ with the pressure $(P - P_m)$ can also be obtained by the slope value of nearly $a_4' = 0.19 - 0.20$ K/MPa at $x = x_m$ from Eq. (15) for all the components of M_1 to M_9 (Table 2), which is a linear variation as plotted in Fig. 2. Thus the increase of pressure $(P - P_m)$ by 1 MPa, changes the temperature $(T - T_m)$ about 0.2 K within the pressure range of 0.1 MPa (atmospheric pressure) to 100 MPa at $x = x_m$ on the basis of the experimental measurements of all the components (M_1 to M_9) for the liquid – solid phase transition in tridecane. This change was nearly 2 K (n-C_{13}, n-C_{14} and n-C_{15}) and 3 K (n-C_{16} and n-C_{17}) per unit change in mass (%) for the linear variation in the temperature $(T - T_m)$ and composition $(x_m - x)$ intervals above the melting point in n-tridecane, as stated previously.

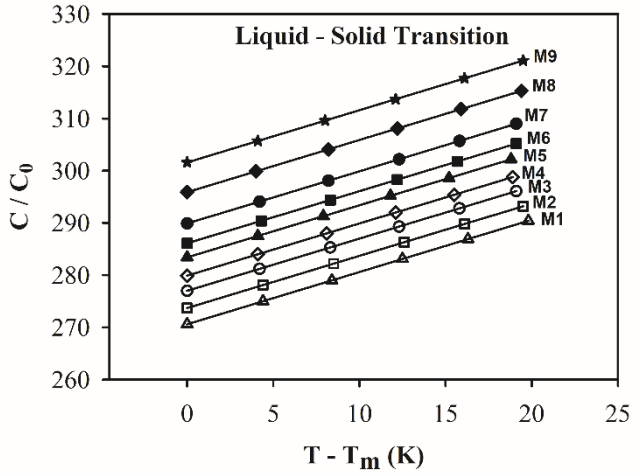

Figure 7. Temperature dependence of the heat capacity C (normalized) for the solid phase, which was calculated according to Eq. (25) at the melting composition ($x = x_m$) using the temperatures, T_m, melting temperatures [4] for liquid – solid transition of various components (M_1 to M_9) of n-tridecane.

Once we calculated the phase diagrams ($T - X$ and $T - P$) for the various mixtures (M_1 to M_9) of n-tridecane (n-C_{13} to n-C_{17}), we were then able to predict the temperature dependence of the order parameter ψ (Fig. 3), inverse susceptibility ${\chi_\psi}^{-1}$ (Fig. 4), free energy F (Fig. 5), entropy S (Fig. 6), the heat capacity C (Fig. 7) and enthalpy H (Fig. 8). Starting from the order parameter ψ, it decreases to zero as the melting temperature is approached from the solid phase (Fig. 3) for the n-tridecane system. The order parameter (normalized) values for all the mixtures (M_1 to M_9) fall onto a single curve as a function of $T_m - T$, as expected according to Eq. (18) with the critical exponent $1/2$. This is the critical exponent value expected from the mean field theory. Thus, at $P = P_m$ and $x = x_m$ for the components of the n-tridecane the order parameter ψ describes the liquid-solid transition (Eq. (18)) on the basis of the phase line equation (Eq. (15)). This can be tested experimentally by the measurements of ψ as a function of $T_m - T$ for various components of n-tridecane. On the other hand, variation of the inverse susceptibility ${\chi_\psi}^{-1}$ is linear with the $T_m - T$ (Fig. 4) according to Eq. (21) at $P = P_m$ for all the compositions (M_1 to M_9). In our calculation of the inverse susceptibility using Eq. (21), we considered the linear term in $T - T_m$ at $P = P_m$ (Eq. (19)) which dominates the behavior of the ${\chi_\psi}^{-1}$ for the liquid – solid phase transition in n- tridecane. This is also consistent with the behavior of the order parameter ψ (Fig. 3) for this mixture.

Regarding the quadratic temperature dependence of the free energy F (Eq. (23)), we obtained that F increases in the solid phase above the melting temperature T_m in the mixtures studied (Fig. 5). From the functional form of F (Eq. (23)), we arrived at a linear variation of the entropy S (Eq. (24)), as plotted in Fig. 6. As the F increases in the solid phase, S increases linearly with the temperature $(T - T_m)$. The heat capacity C also varies linearly (Eq. (25)) above T_m for all the compositions (M_1 to M_9), as plotted separately for each component in Fig. 7. For the second order transitions (solid-solid transitions or transitions in liquid crystals), which is the concern of various theoretical models such as Ising model, Heisenberg model, Potts model, spherical model etc., the entropy S exhibits discontinuity at the critical temperature, T_c. This gives rise to a continuous behaviour of the heat capacity C at the T_c. From the mean field theory, critical behaviour of the C is logarithmic. However, for the liquid-solid transition, which is of the first order, the entropy S and the heat capacity vary linearly with the $T - T_m$, as given in Figs. 6 and 7, respectively.

The heat capacity C (normalized) was plotted as a function of $T - T_m$ above the melting temperature T_m, as plots of the free energy F (Fig. 5), entropy S (Fig. 6) and enthalpy H (Fig. 8). Since the heat capacity was calculated above the T_m, a plot of C/C_0 versus $T - T_m$ provided us to compare all the components M_1 to M_9 with the same slope as a single (universal) curve (with the different C/C_0 values) for the liquid-solid transition in n-tridecane. Starting from the component M_1 up to M_9, the heat capacity (C/C_0) increases linearly above the melting temperature with the same slope value as predicted from the Landau phenomenological model (Eq. (25)), as shown in Fig. 7. This also shows that the heavier component (M_1) in mass (%) has lower heat capacity in magnitude as compared to the lighter one (M_9) which has larger heat capacity for the liquid – solid phase transition in n-tridecane.

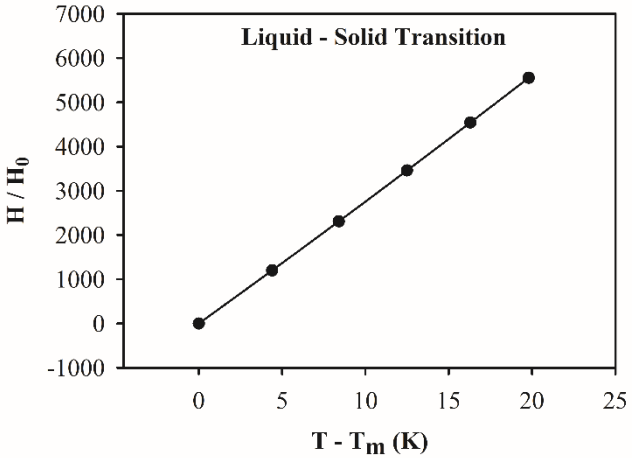

Figure 8. Temperature dependence of the enthalpy H (normalized) for the solid phase, which was calculated according to Eq. (26) at the melting composition ($x = x_m$) using the temperatures, T_m, melting temperatures [4] for liquid – solid transition of various components (M_1 to M_9) of n-tridecane.

As in the case of the free energy F which was described using a quadratic function (Eq. (23)), the enthalpy function was also described quadratically (Eq. (26)) for the liquid – solid transition in the n-tridecane (n-C_{13} to n-C_{17}) with various compositions (M_1 to M_9). It increases as the free energy F (Fig. 5), entropy S (Fig. 6) and the heat capacity C (Fig. 7) above the melting temperature T_m in the solid phase for the liquid – solid transition in tridecane, as expected from the mean field theory. Variation of the enthalpy $H(T)$ with the $T - T_m$ above the melting temperature (T_m), is quadratic according to Eq. (26) for the liquid-solid transition in n-tridecane, as stated previously. However, as shown in Fig. 8 this variation is linear for the temperatures with respect to the melting temperatures T_m (at $P = 0.1$ MPa) for the components M_1 to M_9 (Table 2) within the temperature interval $T - T_m \cong 20$ K according to the six experimental points [4] available for the analysis. This includes the pressure region of 0.1 to ~100 MPa for those components in n-tridecane. Most likely, for the pressures above 100 MPa,

correspondingly at higher temperatures, variation of $H(T)$ with the $T - T_m$ would turn into the quadratic (parabolic) according to Eq. (26) for all the components (M_1 to M_9) regarding the liquid-solid transition in n-tridecane. For our calculations of ψ, ${\chi_\psi}^{-1}$, F, S, C and H as a function of $T - T_m$, the pressure varied with the temperature for the components M_1 to M_9, starting from 0.1 to ~100 MPa on the basis of six experimental points [4], as shown in Fig. 2 ($T - T_m$ versus $P - P_m$).

In our treatment, calculation of the thermodynamic quantities studied here was based on the $T - X$ and $T - P$ phase diagrams of the liquid – solid transition in n-tridecane mixtures. The temperature dependence of the thermodynamic quantities of the order parameter, susceptibility, free energy, entropy, heat capacity and the enthalpy as predicted from the Landau phenomenological model, can be compared with the experimental measurements for the liquid – solid transition in n-tridecane (n-C_{13} to n-C_{19}). Also, the pressure and composition dependence of those thermodynamic functions can be predicted for the liquid – solid transition in those mixtures by using the Landau model as studied here. This can be done by means of Eq. (15) for the $T - P$ dependence at $x = x_m$ (at the melting concentration) and also $T - x$ dependence at $P = P_m$ (at the melting pressure). Those dependences can be substituted into the temperature dependence of the order parameter ψ (Eq. (18)), the inverse susceptibility ${\chi_\psi}^{-1}$ (Eq. (21)), the free energy F (Eq. (23)), entropy S (Eq. (24)), the heat capacity C (Eq. (25)) and the enthalpy (Eq. (26)). One then obtains the pressure and concentration (mole fraction) dependence of those thermodynamic quantities for the liquid-solid transition in n-tridecane. These dependences expected from the Landau phenomenological model can be compared with the experimental data for n-tridecane. This provides the description of the phase transition mechanism in the tridecane system, particularly, the pressure effect on the phase transitions in some more details.

5. Conclusions

$T - X$ and $T - P$ phase diagrams were calculated by the Landau mean field theory for the solid – liquid phase equilibria in n-tridecane using the experimental data from the literature. On the basis of the phase diagrams calculated, the thermodynamic quantities of the order parameter, susceptibility, free energy, entropy, heat capacity and enthalpy were predicted as a function of temperature for the solid – liquid transition in n-tridecane ranging from n-C_{13} to n-C_{17} with various number of components.

Our calculations indicate that the Landau mean field model is adequate to describe the solid – liquid transition in those mixtures. The thermodynamic quantities predicted from the Landau model as studied here, can be compared with the experimental measurements for the n-tridecane when they are available in the literature. As an original work, calculating the phase diagrams and the thermodynamic quantities from the Landau mean field model led us to describe the mechanism of the solid-liquid transition in n-tridecane. Based on the experimental phase diagrams which were described adequately by the present model, predictions of the thermodynamic properties are also acceptable within the model for the solid-liquid transition in this system. Pressure and composition dependence of the thermodynamic quantities can also be studied for the solid – liquid equilibria in n-tridecane under the Landau phenomenological model introduced here. The same approach can be performed for some other mixtures for their solid-liquid transition.

Nomenclature

T	temperature (K)
T_m	melting temperature (K)
x	concentration (mole fraction) (%)
x_m	melting concentration (%)
P	pressure (MPa)
P_m	melting pressure (MPa)
ψ	order parameter
χ_ψ	order parameter susceptibility
F	free energy (J/mol)
C, C_0	heat capacity (J/mol.K)
S, S_0	entropy (J/mol.K)
H, H_0	enthalpy (J/mol)
M	component

References:

[1] M. Milhet, J. Pauly, J.A.P. Coutinho, M. Dirand, J.L. Daridon, "Liquid-solid equilibria under high pressure of tetradecane plus pentadecane and tetradecane plus hexadecane binary systems", *Fluid Phase Equilibria, 235*, 173-181, 2005.

[2] K. Khimeche, Y. Boumrah, M. Benziane, A. Dahmani, "Solid-liquid equilibria and purity determination for binary n-alkane plus naphthalene systems", *Thermochimica Acta, 444*, 166-172, 2006.

[3] G.C. Sekhar, P. Venkatesu, T. Hofman, M.V. P. Rao, "Solid–liquid equilibria of long chain n-alkanes (C18–C28) in N,N-dimethylacetamide", *Fluid Phase Equilibria, 201*, 219-231, 2002.

[4] J.L. Daridon, J. Pauly, M. Milhet, "High pressure solid-liquid phase equilibria in synthetic waxes", *Phys. Chem. Chem. Phys., 4*, 4458-4461, 2002.

[5] U. Domanska, P. Morawski, R. Wierzbicki, "Phase diagrams of binary systems containing n-alkanes, or cyclohexane, or 1-alkanols and 2,3-pentanedione at atmospheric and high pressure", *Fluid Phase Equilibria, 242*, 154-163, 2006.

[6] M. Krishnan, S. Balasubramanian, "n-heptane under pressure: Structure and dynamics from molecular simulations", *J. Phys. Chem. B, 109*, 1936-1946, 2005.

[7] C. Ma, Q. Zhou, F. Li, J. Hao, J. Wang, L. Huang, F. Huang, Q. Cui, "Rotator phases of n-heptane under high pressure: Raman scattering and X-ray diffraction studies", *J. Phys. Chem. C, 115*, 18310-18315, 2011.

[8] I. Denicolo, A.F. Craievich. J. Doucet, "X-ray diffraction and calorimetric phase study of a binary paraffin – C23H48-C24H50", *J. Chem. Phys., 80*, 6200-6203, 1984.

[9] G. Ungar, N. Masic, "Order in the rotator phase of normal alkanes", *J. Phys. Chem., 89*, 1036-1042, 1985.

[10] E. B. Sirota, "Rotator phases of the normal alkanes: An x-ray scattering study", *J. Chem. Phys., 98*, 5809-5824, 1993.

[11] E.B. Sirota, H.E. King, H.H. Shao, D.M. Singer, "Rotator phases in mixtures of n-alkanes", *J. Phys. Chem., 99*, 798-804, 1995.

[12] R.G. Snyder, G. Conti, H.L. Strauss, D.L. Dorset, "Thermally-induced mixing in partially microphase segregated binary m-alkane crystals", *J. Phys. Chem. 97*, 7342-7350, 1993.

[13] E. B. Sirota, "Remarks concerning the relation between rotator phases of bulk n-alkanes and those of langmuir monolayers of alkyl-chain surfactants on water", *Langmuir, 13*, 3849-3859, 1997.

[14] P.K. Mukherjee, "Pressure effect on the rotator-II to rotator I transition of alkanes", *J. Chem. Phys., 130*, 214906, 2009.

[15] D.S. Fu, Y.F. Liu, X. Gao, Y.L. Su, G.M. Liu, D.J. Wang, "Binary n-Alkane Mixtures from Total Miscibility to Phase Separation in Microcapsules: Enrichment of Shorter Component in Surface Freezing and Enhanced Stability of Rotator Phases", *J. Phys. Chem. B, 116*, 3099-3105, 2012.

[16] U. Zammit, M. Marinelli, F. Mercuri, S. Paoloni, "Analysis of the Order Character of the R-II-R-I and the R-I-R-V Rotator Phase Transitions in Alkanes by Photopyroelectric Calorimetry", *J. Phys. Chem. B, 114*, 8134-8139, 2010.

[17] D.S. Fu, Y.F. Liu, G.M. Liu, Y.L. Su, D.J. Wang, "Confined crystallization of binary n-alkane mixtures: stabilization of a new rotator phase by enhanced surface freezing and weakened intermolecular interactions", *Phys. Chem. Chem. Phys., 13*, 15031-15036, 2011.

[18] I. Koljanin, M. Pozar, B. Lovrincevic, "Structure and Dynamics of liquid linear and cyclic alkanes: A molecular Dynamics study", *Fluid Phase Equilibria, 550*, 113237, 2021.

[19] B. He, V. Martin, F. Setterwall," Liquid-solid phase equilibrium study of tetradecane and hexadecane binary mixtures as phase change materials (PCMs) for comfort cooling storage", *Fluid Phase Equilibria, 212*, 97-109, 2003.

[20] P. Morawski, J. A. P. Coutinho, U. Domanska, "High pressure (solid + liquid) equilibria of n-alkane mixtures: experimental results, correlation and prediction", *Fluid Phase Equilibria, 230*, 72-80, 2005.

[21] L. Robles, D. Mondieig, Y. Haget, M. A. Cuevas-diarte, X. Alcobe, "Non isomorphism and miscibility in the solid state: Determination of the equilibrium phase diagram n-octadecane $C_{18}H_{38}$ + n-nonadecane $C_{19}H_{40}$", *Mol. Cryst. Liq. Cryst., 281*, 279-290, 1996.

[22] S.N. Gunasekara, S. Kumova, J.N. Chiu, V. Martin, "Experimental phase diagram of the dodecane-tridecane system as phase change material in cold storage", *Int. J. Ref., 82*, 130-140, 2017.

[23] T. Shen, H. Peng, X. Ling, "Experimental Measurements and Thermodynamic Modeling of Melting Temperature of the Binary Systems n-C11H24-n-C14H30, n-C12H26-n-C13H28, n-C12H26-n-C14H30, and n-C13H28-n-C-15 H-32 for Cryogenic Thermal Energy Storage", *Ind. Eng. Chem. Res., 58*, 15026-15035, 2019.

[24] T. Shen, S. Li, H. Peng, X. Ling, "Experimental study and thermodynamic modeling of solid-liquid equilibrium of binary systems: Dodecane-tetradedcane and tridecane-pentadecane for cryogenic thermal energy storage", *Fluid Phase Equilibria, 493*, 109-119, 2019.

[25] H. Yurtseven, E. Kilit Dogan, "Calculation of the phase diagram of n-alkanes (CnH2n+2) by the Landau mean field theory", *Fluid Phase Equilibria, 556*, 113377, 2022.

[26] H. Yurtseven, T. Emirosmanoglu, O. Tari, "Calculation of the Liquid-Solid Phase Diagram and the Thermodynamic Quantities of the Binary System of Tetradecane and Hexadecane Using the Mean Field Theory", *J. Sol. Chem., 50*, 1335-1362, 2021.

[27] O. Tari, H. Yurtseven, "Calculation of the T-X phase diagram of tetradecane+hexadecane and tetradecane+pentadecane under high pressure by the landau mean field theory", *Fluid Phase Equilibria, 559*, 113499, 2022.

[28] P.K. Mukherjee, "Tricritical behavior of the R-I-R-V rotator phase transition in a mixture of alkanes with nanoparticles", *J. Chem. Phys., 135*, 134505, 2011.